Kursula *et al.*
Low-carbon Materials and Green Construction (2023) 1:28
https://doi.org/10.1007/s44242-023-00031-5

Low-carbon Materials
and Green Construction

ORIGINAL ARTICLE Open Access

Recycling alkali activated slag into artificial aggregate: Influence of particle size distribution of the starting material on granulation

Kalle Kursula[1], Mirja Illikainen[1] and Priyadharshini Perumal[1*]

Abstract

Wet granulation is a potential method to develop artificial aggregates. In this paper, the granulation of recycled alkali-activated slag powders with different particle size (d_{50} ranging between 12.9–127.7 µm) distributions were investigated in order to find how these affect on the engineering properties of the artificial aggregates. Blast furnace slag was added as co-binder in 10–30 wt. % during the granulation process and to enhance the properties, especially mechanical strength. The results show that the particle size of the raw material significantly affects the engineering properties of the produced aggregates, such as the crushing force (19–131.8 N), bulk density, water absorption, porosity and microstructure of the granules. The results show that granulation is a promising method to recycle alkali-activated materials as lightweight aggregates to replace natural aggregates.

Highlights

- New artificial aggregates were produced from recycled alkali activated slag.
- Development of 131.8 N crushing force was achieved using optimal particle size of the raw material.
- It is possible to upcycle alkali activated slag waste to reduce landfill space and contribute circular economy.
- Produced aggregates can be used for example as an aggregate in lightweight concrete produce new green building materials.

Keywords Artificial aggregate, Recycled concrete fines, Concrete powder, Granulation, Alkali activation, Recycling geopolymer

摘要

湿法造粒是一种潜在的人造骨料制备方法。本文研究了不同粒径分布的再生碱激发矿渣粉(d_{50}介于12.9–127.7 µm)对人造骨料性能的影响。此外，在造粒过程中掺入质量分数为10–30%的高炉矿渣作为辅助胶凝材料，以提高其性能，特别是力学强度。试验结果表明，原料粒径对制备的人造骨料的性能产生了显著影响，如压碎力(19–131.8N)、堆积密度、吸水率、孔隙率和微观结构等。因此，将回收的碱活性材料进行造粒成轻质骨料并替代天然骨料是一种很有前景的方法。

关键词 人造骨料，再生混凝土砂粉混料，混凝土微粉，造粒，碱激发，再生地聚合物

*Correspondence:
Priyadharshini Perumal
Priyadharshini.perumal@oulu.fi
Full list of author information is available at the end of the article

Graphical Abstract

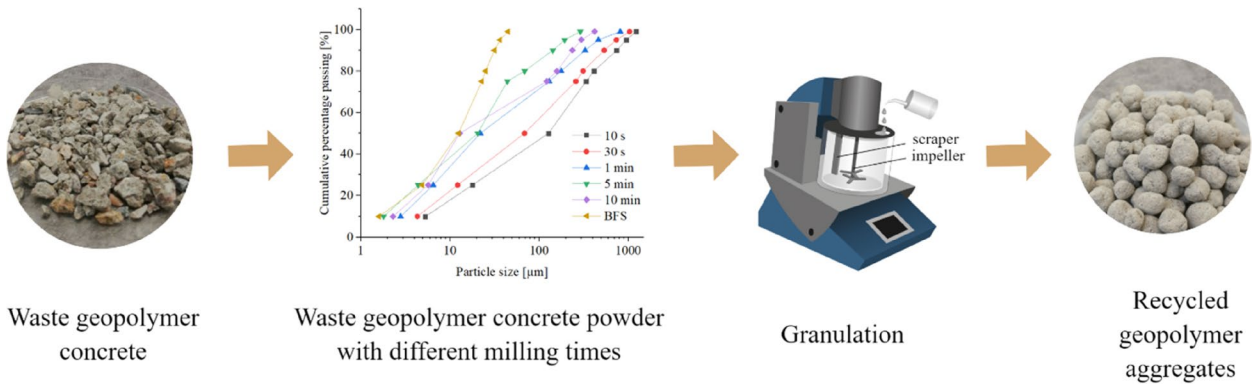

1 Introduction

Cement production is one of the major contributors to global warming due to the enormous carbon dioxide (CO_2) and greenhouse gas emissions [1]. There is wide interest to develop alternative low-carbon concretes and binders. The most straightforward way to decrease concrete CO_2 emissions is to use supplementary cementitious materials (SCMs) to partially replace ordinary Portland cement [2]. There is a growing interest to develop concrete where cement is totally replaced with alternative binder. One of the most important achievements in this research area is the development of geopolymer concrete (GPC) [3, 4]. Geopolymer concrete is recommended as a suitable alternative to the OPC-based concrete because of good engineering properties and low carbon footprint [5]. In the production of GPC, aluminosilicate materials, like industrial by-products and wastes such as fly ash and ground granulated blast furnace slag (BFS), are activated using an alkaline solution such as sodium hydroxide (NaOH) or sodium silicate (Na_2SiO_3). [6]. The GPC has been reported to have significant environmental benefits. However, the recycling and reuse of GPC has received little attention in the literature.

Huge amount of concrete waste is produced annually, and the portion of GPC waste in the total construction and demolition waste (CDW) amount will increase in the next decades, if GPC will replace the use of Portland cement concrete [7]. Therefore, studying the feasibility and challenges dealing with the GPC waste needs particular attention. The available literature on GPC recycling is limited to the use of recycled geopolymer aggregates as coarse aggregates for Portland cement concrete [8] and the use of recycled concrete aggregate in a geopolymer concrete matrix [9]. However, there is currently a gap in knowledge about recyclability of recycled alkali-activated slag (AAS) powder and investigating it can provide a profitable replacement for natural aggregates and help to evaluate the sustainability of GPC.

Granulation is a potential technology to produce artificial aggregates that can be alternative materials to natural aggregates (NAs). There is also a lack of NAs so replacing them by artificial aggregates can alleviate this problem also. It could be also a viable way to investigate the recyclability of waste AAS powder. Various wastes have been used in the literature to manufacture artificial aggregates, Like as fly ash and steel slag [10–14]. In this study, ground granulated blast furnace slag (BFS) was chosen to be the co-binder, because it is an industrial waste from pig iron production, and it is widely used as a precursor in the production of geopolymers [15].

Therefore, the main focus of this work is to study the recyclability of recycled AAS powder by producing artificial aggregates for use in lightweight concrete through granulation. Recycled AAS powder was used as binder in different particle sizes in order to examine the influence of the particle size on the properties of aggregates. In addition, different amount of co-binder is used. Physical, mechanical, mineralogical and microstructural properties are specifically investigated and evaluated in order to study the effect of particle size on the granulation process and differences of the different particle size and co-binder amount.

2 Materials and methods

2.1 Materials

In this study the discarded geopolymer paste samples sourced from the research study made by [16] was used for recycling (referred hereafter as recycled geopolymer). The geopolymer paste used were made using BFS as a binder and sodium metasilicate as the solid activator. BFS was supplied from Finnsementti (Finland). Those geopolymer paste blocks were cured at ambient condition at 23°C and then

placed to the freezer at the temperature from -5°C to -20°C, as the aim of the study was to understand the effects of subzero temperatures on properties of geopolymer in order to use them as construction materials in cold climatic regions [16]. The chemical composition of the crushed recycled geopolymer was analyzed by X-Ray Fluorescence (XRF) spectrometer (Omnian Panalytics). The chemical content of the materials is given in Table 1. As seen, the main oxide compounds are SiO_2, CaO, Al_2O_3, MgO, Na_2O and SO_3.

The geopolymer blocks were crushed by hammer and milled until the fine particles passed the 2 mm sieve. This procedure is generally used in the other studies on granulation [17]. After that, six different milling times were used to produce recycled AAS powder with different particle size distribution. Vibratory disc mills (RS200 Retcsh) was used in the milling process. After the milling process, the particle size distribution was measured by laser diffraction method (Fraunhofer method) and wet procedure in isopropanol by particle size analyzer (Beckman Coulter LS 13 320). The milling times were 10 s, 30 s, 1 min, 5 min and 10 min and the the corresponding particle size d_{50} of the milled batches were 127.7 µm, 68.6 µm, 21,9 µm, 20,5 µm and 12.9 µm, respectively. (Fig. 1). The typical particle size is below 200 µm but there are some large particles also occurring. Surprisingly, there is not big difference in the corresponding particle size d_{50} between the powder milled for 1 min and 5 min.

Table 1 The chemical composition of recycled alkali-activated slag (AAS) powder and blast furnace slag (BFS) used in the experiment

Chemical composition (Wt.%)	Recycled AAS powder	BFS
SiO_2	57.4	32.3
Fe_2O_3	0.4	1.2
Al_2O_3	3.6	9.6
TiO_2	0.5	2.2
CaO	13.7	38.5
MgO	3.1	10.2
SO_3	1.3	4.0
K_2O	0.6	0.5
Na_2O	2.7	0.5
Others	16.7	1.0

X-ray diffraction (XRD) analysis was done with a SmartLab analyzer (Rigaku). XRD analysis used CuKα radiation with scan speed of 4°/min, scan range of 5–120° and step width of 0.02°.

Figure 2 shows the X-ray diffraction patterns of different materials used. According to the X-ray diffraction analysis, the recycled AAS powder contained quartz (SiO_2), calcite ($CaCO_3$) and portlandite ($Ca(OH)_2$). For the milled AAS, an increase in the amount of quartz and decrease in calcite is observed. Ettringite is formed after milling that may related to the reduction in the amount of calcite in the AAS:

2.2 Granulation of milled AAS

Blast furnace slag with 10% sodium silicate was used as the co-binder in the granulation. BFS was obtained from the Finnsementti (Finland) and it had the density of 2.93 g/cm^3 and d_{50} value of 10.8 µm. Commercially available granular sodium silicate (Na_2SiO_3) powder (Sikalon N 601, 99% purity) was used in this study. The sodium silicate was in the granulate form, so it was milled in

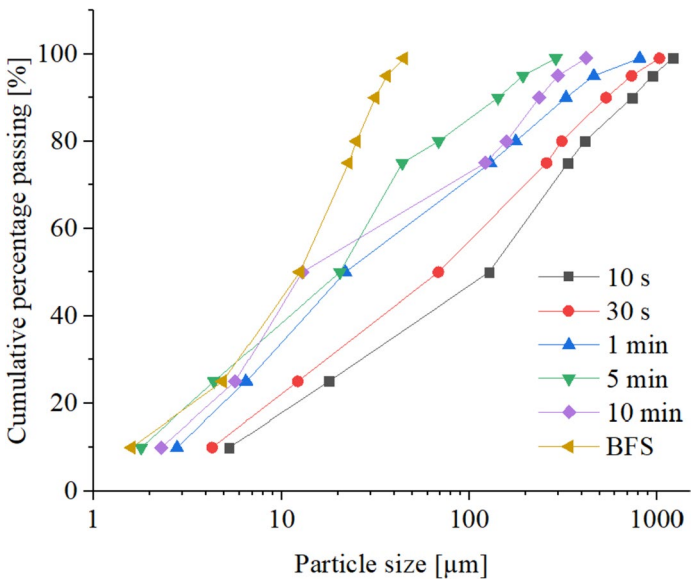

Fig. 1 Particle size distributions of the milled alkali activated slag powder

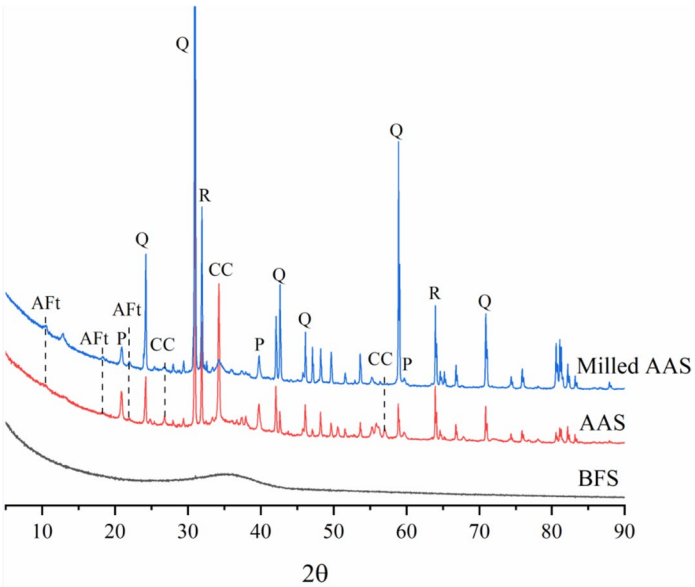

Fig. 2 XRD patterns for blast furnace slag, recycled AAS powder and recycled AAS powder milled for 1 min with 30% BFS. AFT: Ettringite, Q: Quartz (SiO_2), P: Portlandite ($Ca(OH)_2$), CC: Calcite ($CaCO_3$)

vibratory disc mill to make it in powder form. 100 g of sodium silicate granules were milled two times, first 1.5 min at speed of 1500 rpm and then 3 min at 700 rpm. Four different mix designs were prepared, having the co-binder amounts of 0%, 10%, 20% and 30%.

Therefore, 20 batches of granules with 5 different particle size and 4 different co-binder amount were prepared, and they were granulated using de-ionized water. A high-shear granulator (Eirich R-02) was used in this study. The granulator is equipped with rotating drum with an impeller. The volume of the drum was 13,000 cm^3 and the diameter of the drum was 14 cm. During the granulation process, the tilt angle of the granulator was 40° and the rotating speed was 300 rpm, based on the preliminary studies [18]. The granulation process was carried out by weighing 200 g of each milled batch that was added to the drum. The impeller and drum were switched on, and de-ioneized water was added by drops on the powder bed rotating inside the granulator. About 250 g of water was added to each batch in order to produce granules with the diameter between 5–8 mm. After the granulation process, each batch of the granules was sealed in the air-tight plastic bags and cured in the room condition for seven days until further analysis.

2.3 Characterization methods

The granule strength was determined using the single granule crushing method [19, 20]. The crushing force of the granules at the age of 7 days was measured by testing machine (Zwick-Roell 100 kN) with maximum load of 100 kN and a loading rate of 2.4 kN/s. For each granulation batch, at least ten randomly selected granules were tested, and the average was calculated that was regarded as the representative value of the strength. The diameter of a granule was measured before the granule was placed in a testing machine. In addition, the standard deviation between specimens was calculated and presented as error bars in the results. The crushed granules were used in the mineralogical and microscopical analyses, and therefore, the hydration reaction was stopped by solvent exchange using isopropanol [21].

The bulk density and water absorption of the granules were determined according to the European Standard EN 1097–3 of tests of mechanical and physical properties of aggregates. The bulk density was calculated using Eq. (1):

$$\rho = \frac{m}{V} \tag{1}$$

where ρ is the bulk density [kg/m^3], m is the mass [kg] and V is the volume [m^3].

The water absorption is a fundamental indicator of the granule durability. An oven with temperature of 100°C was used for drying the granules for 24 h, and in the next step, the granules were immersed in water at room temperature for 24 h. The water absorption was calculated using the Eq. (2):

$$\textit{Water absorption}\ (\%) = \frac{B - A}{B} \times 100 \tag{2}$$

where A is the granules mass after drying in oven [kg] and B is the surface-dried mass after immersion [kg].

Porosity of the granules was estimated based on the values of bulk density and particle density. The particle

density was measured by analyzing the powdered granule samples using helium gas pycnometer (Micromeritics). The porosity was calculated using the Eq. (3):

$$P(\%) = (1 - \frac{\rho_B}{\rho_P}) \times 100 \quad (3)$$

where P is porosity [%], ρ_B is the bulk density [kg/m^3] and ρ_P is the particle density [kg/m^3].

The width of the particle size distribution (W_{PSD}) was calculated using Eq. (4):

$$W_{PSD} = \frac{d_{90} - d_{10}}{d_{50}} \quad (4)$$

where d_{90}, d_{50} and d_{10} are the particle sizes in micrometers corresponding to the 90%, 50% and 10% values in the cumulative volumetric size distribution, respectively.

X-ray diffraction (XRD) analysis was done with a SmartLab analyzer (Rigaku). XRD analysis used CuKα radiation with scan speed of 4°/min, scan range of 5–120° and step width of 0.02°. Internal standard was used by adding 10 wt% of rutile (TiO_2).

In addition, the morphologies of the granules were studied by optical microscopy. Optical microscopy studies were done using a Leica DFC420 camera (Leica MZ6).

3 Results and discussion

3.1 Crushing value

The width of the particle size distributions were calculated according to the Eq. (4) and they were 7.78 µm, 5.76 µm, 18.21 µm, 6.87 µm and 14.89 µm for milling times of 10 s, 30 s, 1 min, 5 min and 10 min, respectively. Recycled AAS powder (RGP) having W_{PSD} of 14.89 µm had the highest crushing force among the five different milling times used. RGP (1 min milled) granules achieved an optimal average crushing force of 131.8 N with 30% of co-binder (Fig. 3). Generally, the higher amount of co-binder resulted in a higher strength of the aggregate as expected. Surprisingly, the aggregates produced from AAS powder milled for 30 s gained the lowest strength (19 N). The strength development of those granules does not show any changes even with the addition of the co-binder. In contrast, aggregates produced from AAS powder milled for 10 s and 1 min gained 126.5% and 20.3% increase in strength, respectively, when co-binder was added from 0 to 30%. The huge difference in the strength of aggregates granulated from AAS powder milled for 1 min compared to others was obviously caused by the optimal particle size distribution of the starting material, that gave a good packing for the granules and impacted the development of micro-structure.

3.2 Bulk density

The bulk densities of the aggregates were in the range 977 kg/m^3 to 1149.5 kg/m^3 (Fig. 4). The density of aggregates produced from 1 min milling time was the highest, especially with the BFS ranges from 1149.7 kg/m^3 to 1418.9 kg/m^3 (Fig. 4). Other aggregates had lower and quite similar bulk density values. Increasing milling time longer than 1 min leads to a drop in the loose bulk density values, probably because the material is very fine then. It was obvious that the aggregates having BFS as co-binder had slightly higher density than those without it. It must

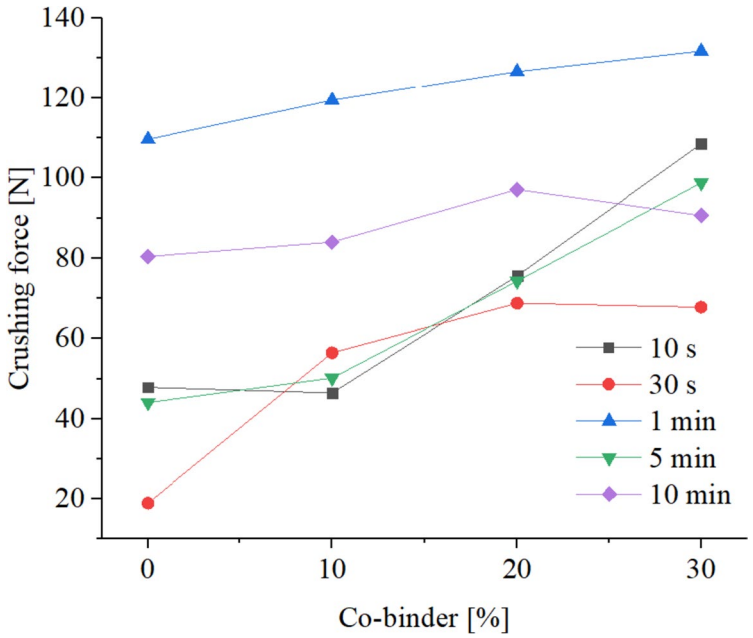

Fig. 3 Crushing strength of the aggregates

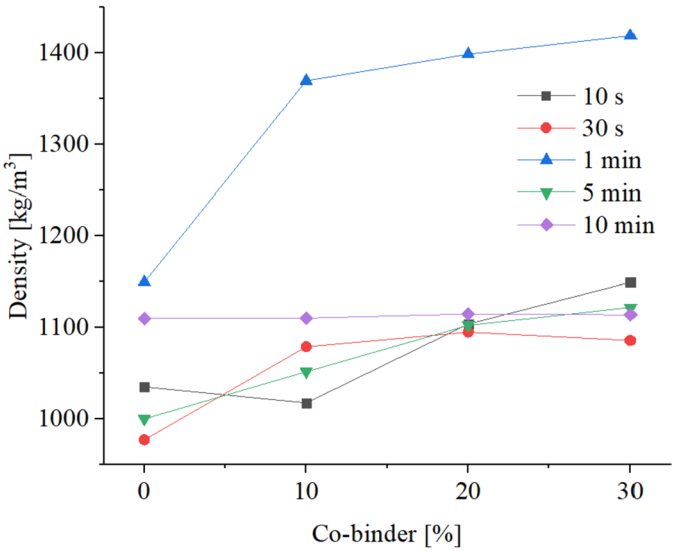

Fig. 4 Loose bulk density of the aggregates

be noticed that all the granules except 1 min milling time with 10%, 20% and 30% BFS can be classified as lightweight aggregates according to the standard EN 13055–1 (1200 kg/m^3). In addition, the effect of binder content can be only observed for the granules produced from powder milled for 1 min. The variability in the bulk density values is probably related to their different hydration degree and particle size. Generally, the crushing force and bulk density have relatively good consistency. In addition, the higher density is related to the lower water absorption and porosity. Probably the improvement in the density of 1 min aggregates was related to the packing effect that effectively fills the pores and makes the aggregate denser, when BFS was added.

3.3 Water absorption

In terms of water absorption, the granules showed variable values ranging from 21.6% to 0.7% after immersion for 24 h (Fig. 5). The differences in the water absorption are related to the different co-binder amount and raw

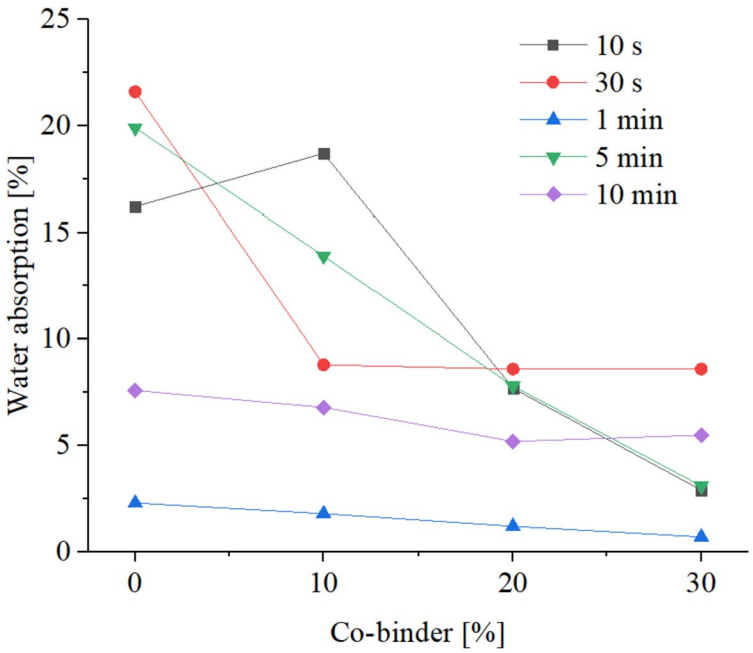

Fig. 5 Water absorption of the aggregates at 7th day of curing

material reactivity [22]. The granules that did not contain any co-binder had a much higher water absorption rate except the 1 min and 10 min samples. Generally, when the binder content increases the water absorption decreases, as expected. The use of BFS as co-binder lowered the porosity and developed the dense microstructure of the granules, because of better pozzolanic and hydration reactions [22]. The water absorption values are in the good consistency with the density results. On the other hand, the water absorption values had wider limits compared to density (0.7–21.6%).The 1 min granules had the lowest water absorption values ranging from 2.3% to 0.7%. Probably granules produced from this particle size had tight packing on the granule surface that prevents water penetration [23].

3.4 Porosity

The good compaction during granulation resulted in lower porosity (Fig. 6). The porosity of the granules ranged from 9.9% to 0.1%. It can be seen that 1 min granules had lower porosity than the other ones. The porosity results are in consistency with the crushing force, density and water absorption results. Lower porosity resulted in higher crushing force and density. The higher porosity is attributed to the higher water absorption that was expected because more porous granules can absorb more water. It seems that the porosity reduces when the BFS content increases. Probably the use of BFS as co-binder can fill the pores of aggregates and cover the surface of particles leading to lower porosity of granules.

3.5 Width of the particle size distribution

The strength of the artificial aggregates correlates quite well with the particle size distribution of the recycled AAS (Fig. 7). During the granulation, the starting particle size of the material affects on the size and strength of the final aggregates [24]. The smaller particles enhance the granulation process by giving more nucleation material for the agglomeration. In addition, wider particle size distribution can affect on the strength of the granules by better packing effect [25]. The particle size distribution width was 18.21 µm and 14.89 µm for the milling times of 1 min and 10 min, respectively, that yielded in the highest strength of the aggregates. In comparison, the particle size distribution width was only 5.76 µm, 6.87 µm and 7.78 µm for the milling times of 30 s, 5 min and 10 s, respectively.

3.6 Microstructure

One min granules appeared with a relatively homogeneous layer, while the other granules appeared to be composed of numerous small pores (Fig. 8a-h). It can be also observed that the addition of BFS as a co-binder enhanced the microstructure of the granules by covering the aggregate surface (Fig. 8c-f). The optical microscopy study revealed that especially 30 s-0%BFS granules had a very irregular and loose structure (Fig. 8b). Generally, the surfaces of the granules are relatively rough, probably due to the hydration products formation that make the surface of the aggregate very rough [26]. It can be noticed that the 1 min-30%BFS granule surface is very smooth, which presumably improved the bonding strength and crushing force of the aggregate. The microstructural characterization is in good accordance with the mechanical testing results since the large amount of pores leads to weaker strength of the granules and higher water absorption.

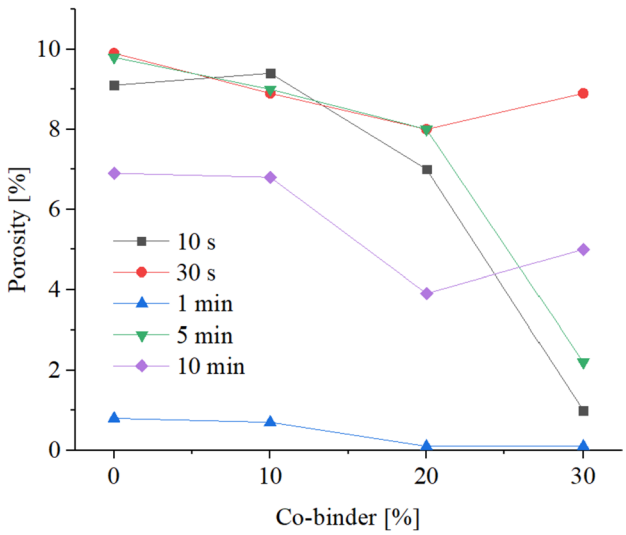

Fig. 6 Porosity of the granules

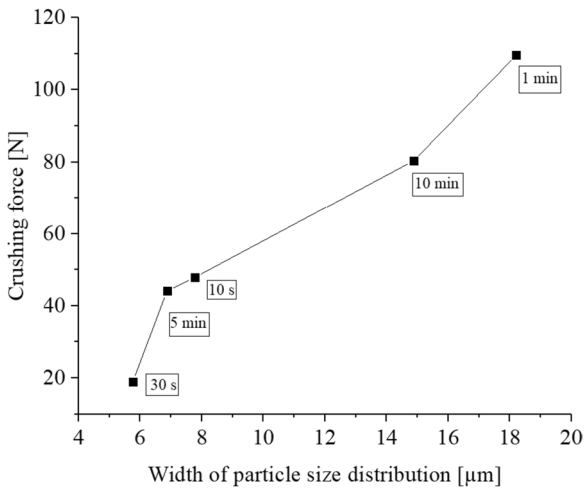

Fig. 7 The correlation between particle size distribution width and crushing force

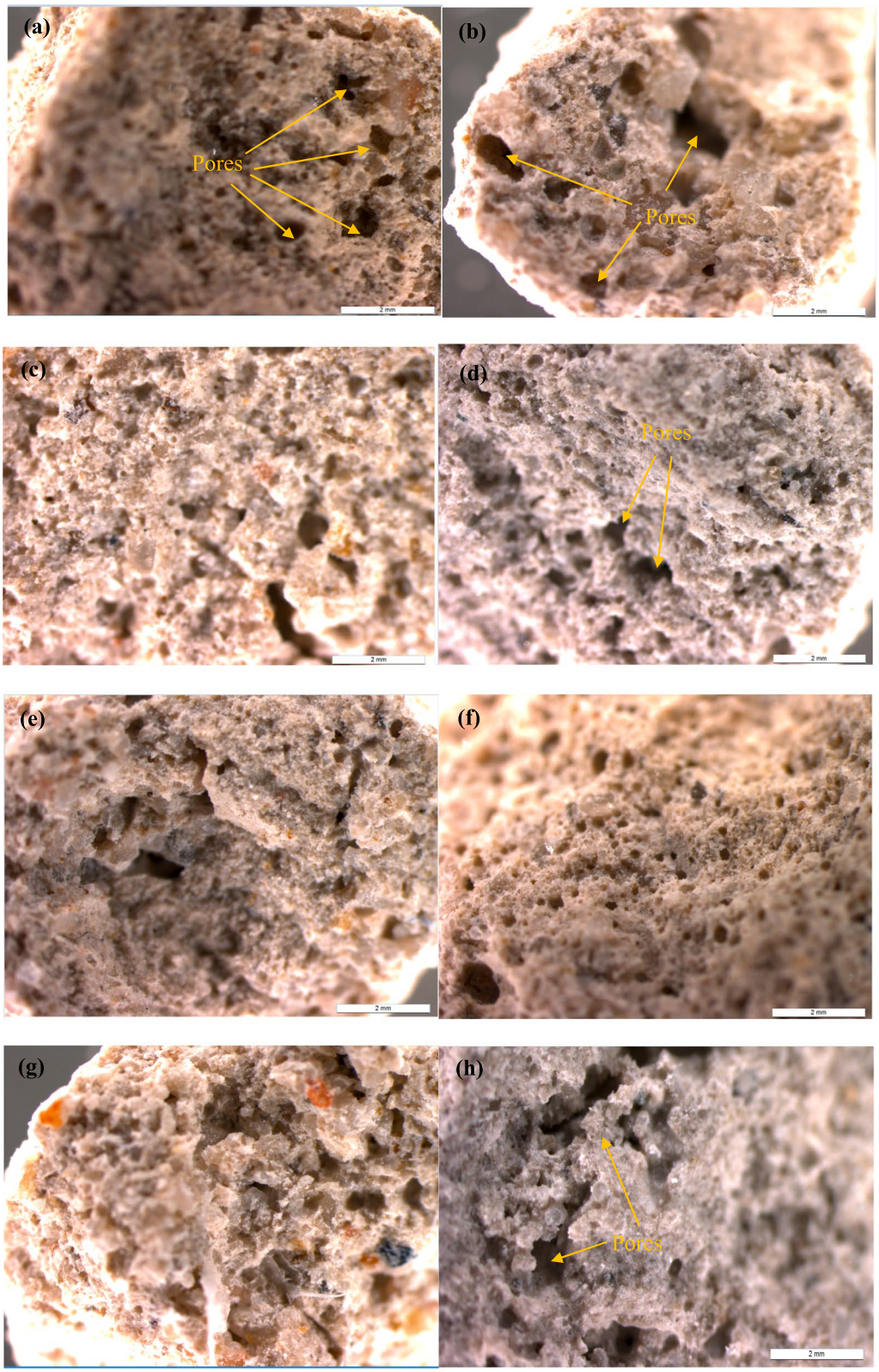

Fig. 8 Optical microscope images of (**a**) 10 s-0%BFS, (**b**) 30 s-0%BFS, (**c**) 1 min-0%BFS, (**d**) 1 min-10%BFS, (**e**) 1 min-20%BFS, (**f**) 1 min-30%BFS, (**g**) 5 min-0%BFS and (**h**) 10 min-0%BFS granules

4 Conclusions

In this investigation, the recycled AAS powder with blast furnace slag (BFS) was used to manufacture artificial aggregates by granulation process. The effects of different particle sizes of AAS powder and co-binder amount on the properties of the produced aggregates were studied. It was observed that the properties of the aggregates depend on the particle size of the recycled AAS powder, as well as the amount of the BFS as a co-binder. The feasibility of using recycled AAS powder as a raw material for artificial aggregates was evaluated especially in terms of crushing force, bulk density, water absorption and porosity.

Based on the results obtained in this study, the following conclusions can be drawn:

Using recycled AAS powder milled for 1 min can significantly increase the crushing force of the granules varying between 109.6–131.8 N. This may be related to the higher particle size distribution width that enhances the mechanical properties of the aggregates by better particle packing effect. Also, In addition, using blast furnace slag as a co-binder is an effective way to enhance the performance of the artificial aggregates produced from the recycled AAS powder. Therefore, the granulation method could be an effective way to treat these recycled materials and produce high-strength granules for the lightweight aggregate applications. The loose bulk density and water absorption values also were suitable in most cases for the civil engineering purposes. Therefore, the developed granulated artificial aggregates have a great potential to be used in low density lightweight concrete to produce sustainable and green building material.

Acknowledgements
The authors acknowledge the financial support received for the project DeConcrete Eco-Efficient Arctic technologies cooperation funded by kolarctic CBC initiative of European Union (KO 4068). XRD analysis was performed at the Center of Microscopy and Nanotechnology (University of Oulu). The authors would like to thank Jarno Karvonen and Elisa Wirkkala for their assistance with the laboratory experiments.

Authors' contributions
All authors contributed to the study conception and design. Material preparation, data collection and analysis were performed by Kalle Kursula and Priyadharshini Perumal. The first draft of the manuscript was written by Kalle Kursula and all authors commented on previous versions of the manuscript. All authors read and approved the final manuscript.

Availability of data and materials
The datasets generated during and/or analysed during the current study are available from the corresponding author on reasonable request.

Declarations

Ethics approval and consent to participate
This article does not contain any studies with human participants or animals performed by any of the authors. This study was done according to ethical standards.

Consent for publication
Not applicable.

Competing interests
Priyadharshini Perumal is one of the Editor for the special issue, "Advances in sustainable materials and structures" in Low-carbon Materials and Green Construction and was not involved in the editorial review, or the decision to publish, this article. All authors declare that there are no other competing interests. The authors have no relevant financial or non-financial interests to disclose.

Author details
[1]Fibre and Particle Engineering Research Unit, Faculty of Technology, University of Oulu, PO Box 4300, Oulu 90014, Finland.

Received: 22 May 2023 Revised: 4 September 2023 Accepted: 2 October 2023
Published online: 29 November 2023

References

1. Ali, M. B., Saidur, R., & Hossain, M. S. (2011). A review on emission analysis in cement industries. *Renewable and Sustainable Energy Reviews, 15*(5), 2252–2261. https://doi.org/10.1016/j.rser.2011.02.014
2. Flatt, R. J., Roussel, N., & Cheeseman, C. R. (2012). Concrete: an eco material that needs to be improved. *Journal of the European Ceramic Society, 32*(11), 2787–2798. https://doi.org/10.1016/j.jeurceramsoc.2011.11.012
3. Akbarnezhad, A., & Xiao, J. Z. (2017). Estimation and minimization of embodied carbon of buildings: a review. *Buildings, 7*(4), 5. https://doi.org/10.3390/buildings7010005
4. Duxson, P., Fernández-Jiménez, A., Provis, J. L., Lukey, G. C., Palomo, A., & van Deventer, J. S. J. (2007). Geopolymer technology: the current state of the art. *Journal of Materials Science, 42*(9), 2917–2933. https://doi.org/10.1007/s10853-006-0637-z
5. Singh, N. B., & Middendorf, B. (2020). Geopolymers as an alternative to Portland cement: an overview. *Construction and Building Materials, 237*, 117455. https://doi.org/10.1016/j.conbuildmat.2019.117455
6. Duxson, P., & Provis, J. L. (2008). Designing precursors for geopolymer cements. *Journal of the American Ceramic Society, 91*(12), 3864–3869. https://doi.org/10.1111/j.1551-2916.2008.02787.x
7. El-Naggar, K. A. M., Amin, Sh. K., El-Sherbiny, S. A., & Abadir, M. F. (2019). Preparation of geopolymer insulating bricks from waste raw materials. *Construction and Building Materials, 222*, 699–705. https://doi.org/10.1016/j.conbuildmat.2019.06.182
8. Mesgari, S., Akbarnezhad, A., & Xiao, J. Z. (2020). Recycled geopolymer aggregates as coarse aggregates for Portland cement concrete and geopolymer concrete: effects on mechanical properties. *Construction and Building Materials, 236*, 117571. https://doi.org/10.1016/j.conbuildmat.2019.117571
9. Shi, X. S., Collins, F. G., Zhao, X. L., & Wang, Q. Y. (2012). Mechanical properties and microstructure analysis of fly ash geopolymeric recycled concrete. *Journal of Hazardous Materials, 237–238*, 20–29. https://doi.org/10.1016/j.jhazmat.2012.07.070
10. Colangelo, F., Messina, F., & Cioffi, R. (2015). Recycling of MSWI fly ash by means of cementitious double step cold bonding pelletization: technological assessment for the production of lightweight artificial aggregates. *Journal of Hazardous Materials, 299*, 181–191. https://doi.org/10.1016/j.jhazmat.2015.06.018
11. Gesoğlu, M., Özturan, T., & Güneyisi, E. (2007). Effects of fly ash properties on characteristics of cold-bonded fly ash lightweight aggregates. *Construction and Building Materials, 21*(9), 1869–1878. https://doi.org/10.1016/j.conbuildmat.2006.05.038
12. Gunning, P. J., Hills, C. D., & Carey, P. J. (2009). Production of lightweight aggregate from industrial waste and carbon dioxide. *Waste Management, 29*(10), 2722–2728. https://doi.org/10.1016/j.wasman.2009.05.021
13. Morone, M., Costa, G., Polettini, A., Pomi, R., & Baciocchi, R. (2014). Valorization of steel slag by a combined carbonation and granulation treatment. *Minerals Engineering, 59*, 82–90. https://doi.org/10.1016/j.mineng.2013.08.009

14. Pang, B., Zhou, Z. H., & Xu, H. X. (2015). Utilization of carbonated and granulated steel slag aggregate in concrete. *Construction and Building Materials, 84*, 454–467. https://doi.org/10.1016/j.conbuildmat.2015.03.008
15. Krivenko, P. (2017). Why alkaline activation – 60 years of the theory and practice of alkali-activated materials. *Journal of Ceramic Science and Technology, 8*, 323–334. https://doi.org/10.4416/JCST2017-00042
16. Alzaza, A., Ohenoja, K., & Illikainen, M. (2021). One-part alkali-activated blast furnace slag for sustainable construction at subzero temperatures. *Construction and Building Materials, 276*, 122026. https://doi.org/10.1016/j.conbuildmat.2020.122026
17. Iveson, S. M., Litster, J. D., & Ennis, B. J. (1996). Fundamental studies of granule consolidation part 1: effects of binder content and binder viscosity. *Powder Technology, 88*(1), 15–20. https://doi.org/10.1016/0032-5910(96)03096-3
18. Kursula, K., Perumal, P., Ohenoja, K., & Illikainen, M. (2022). Production of artificial aggregates by granulation and carbonation of recycled concrete fines. *Journal of Material Cycles and Waste Management, 24*, 2141–2150.
19. Arslan, H., & Baykal, G. (2006). Utilization of fly ash as engineering pellet aggregates. *Environmental Geology, 50*(5), 761–770. https://doi.org/10.1007/s00254-006-0248-7
20. Li, Y. D., Wu, D. F., Zhang, J. P., Chang, L., Wu, D. H., Fang, Z. P., & Shi, Y. H. (2000). Measurement and statistics of single pellet mechanical strength of differently shaped catalysts. *Powder Technology, 113*(1–2), 176–184. https://doi.org/10.1016/S0032-5910(00)00231-X
21. Nguyen, H., Kunther, W., Gijbels, K., Samyn, P., Carvelli, V., Illikainen, M., & Kinnunen, P. (2021). On the retardation mechanisms of citric acid in ettringite-based binders. *Cement and Concrete Research, 140*, 106315. https://doi.org/10.1016/j.cemconres.2020.106315
22. Gesoğlu, M., Güneyisi, E., & Öz, H. Ö. (2012). Properties of lightweight aggregates produced with cold-bonding pelletization of fly ash and ground granulated blast furnace slag. *Materials and Structures, 45*(10), 1535–1546. https://doi.org/10.1617/s11527-012-9855-9
23. Kockal, N. U., & Ozturan, T. (2011). Characteristics of lightweight fly ash aggregates produced with different binders and heat treatments. *Cement and Concrete Composites, 33*(1), 61–67. https://doi.org/10.1016/j.cemconcomp.2010.09.007
24. Cioffi, R., Colangelo, F., Montagnaro, F., & Santoro, L. (2011). Manufacture of artificial aggregate using MSWI bottom ash. *Waste Management, 31*(2), 281–288. https://doi.org/10.1016/j.wasman.2010.05.020
25. Ren, P., Ling, T. C., & Mo, K. H. (2021). Recent advances in artificial aggregate production. *Journal of Cleaner Production, 291*, 125215. https://doi.org/10.1016/j.jclepro.2020.125215
26. Gesoğlu, M., Özturan, T., & Güneyisi, E. (2006). Effects of cold-bonded fly ash aggregate properties on the shrinkage cracking of lightweight concretes. *Cement and Concrete Composites, 28*(7), 598–605. https://doi.org/10.1016/j.cemconcomp.2006.04.002

Publisher's Note